

On the Stabilization of Gold Nanoparticles over Silica-Based Magnetic Supports Modified with Organosilanes

Rafael L. Oliveira,^[a] Daniela Zanchet,^[b, c] Pedro K. Kiyohara,^[d] and Liane M. Rossi^{*[a]}

Abstract: The immobilization of gold nanoparticles (Au NPs) on silica is made possible by the functionalization of the silica surfaces with organosilanes. Au NPs could only be stabilized and firmly attached to silica-support surfaces that were previously modified with amino groups. Au NPs could not be stabilized on bare silica surfaces and most of the NPs were then found in

the solution. The metal–support interactions before and after the Au NP formation, observed by X-ray absorption fine structure spectroscopy (XAFS), indicate a stronger interaction of gold-

(III) ions with amino-modified silica surfaces than with the silanol groups in bare silica. An amino-modified, silica-based, magnetic support was used to prepare an active Au NP catalyst for the chemoselective oxidation of alcohols, a reaction of great interest for the fine chemical industry.

Keywords: gold • nanoparticles • organosilanes • silica • X-ray absorption spectroscopy

Introduction

The selective oxidation of alcohols to yield aldehydes, ketones, carboxylic acids, and their derivatives is one of the most important reactions in organic chemistry.^[1] The chemoselective oxidation, by discrimination of oxygen-sensitive functionalities such as carbon–carbon double-bond functional groups and hydroxyl groups—for example, the oxidation of allylic alcohols to α,β -unsaturated carbonyl compounds—is very interesting for the fine chemical industry. In general, the use of metal-based oxidants containing osmium, chromium, and manganese, which form stoichiometric amounts of residues, is no longer tolerable.^[2] The use of molecular oxygen in oxidation reactions has been encouraged, because water is theoretically the only co-product. Many catalysts based on metal nanoparticles (NPs), such as palladium, silver, and platinum, have been developed to make the use of this “green oxidant” possible.^[3–13] More recently, Au NPs, though less active, have shown better selectivity in multi-

functional alcohol oxidation than other metals and alloys.^[14–16] Pioneers in this field, Corma et al.^[17] performed very interesting mechanistic studies on the selective oxidation of alcohols by Au NPs. The systematic study of the influence of the Au NP size, the nature of the support, and the catalyst preparation procedure has contributed to the design of more active gold catalysts. Much progress in this field has led to improved catalytic activities,^[18–31] however, the use of traditional inorganic supports still requires workup procedures, such as filtration or centrifugation, to collect the supported catalysts. Multifunctional nanomaterials containing magnetic NPs have emerged as a new class of catalyst supports with the great advantage of being readily collected and recovered from the reaction mixture by using an external magnetic field. Catalyst separation and recycling is achieved by simple magnetic separation without the need of filtration, centrifugation, or any other time and energy-consuming workup procedure.^[32–39] We have successfully applied magnetic separation to the easy recovery, recycle, and reuse of Pd,^[32,33] Rh,^[34] Ru,^[35] and Pt^[36] NPs for application in hydrogenation and oxidation reactions. In these examples, a silica-coated, magnetic NP catalyst support was used.

In general, supported Au NPs are prepared by the deposition–precipitation or co-precipitation procedure and the NP sizes are tentatively adjusted by varying experimental parameters, such as the pH, reducing agent, concentration of precursors in solution, and temperature of calcination. However, the surfaces of acid or hydrophobic supports, such as SiO₂, WO₃, and active carbon, are not suitable for the deposition of anionic species and usually lead to large >20 nm supported Au NPs. In such acid supports, other synthetic methods are required to produce small Au NPs, such as deposition of pre-synthesized colloidal gold,^[40–44] chemical vapor deposition,^[45] or atomic beam deposition.^[46] In general, these methods involve many steps, the use of expensive sta-

[a] Dipl.-Chem. R. L. Oliveira, Prof. Dr. L. M. Rossi
Instituto de Química, Universidade de São Paulo
Av. Prof. Lineu Prestes 748 São Paulo
05508-000 São Paulo (Brazil)
Fax: (+55)1138155579
E-mail: lrossi@iq.usp.br

[b] Prof. Dr. D. Zanchet
Laboratório Nacional de Luz Síncrotron, CP 6192
Campinas, 13083-970 São Paulo (Brazil)

[c] Prof. Dr. D. Zanchet
Instituto de Química, Universidade Estadual de Campinas
CP 6154 Campinas, 13083-970, São Paulo (Brazil)

[d] Prof. Dr. P. K. Kiyohara
Instituto de Física, Universidade de São Paulo, CP 66318
05315-970 São Paulo (Brazil)

Supporting information for this article is available on the WWW under <http://dx.doi.org/10.1002/chem.201002251>.

bilizing agents and precursors, and in some cases, require sophisticated equipment. All these factors limit the applications of Au NPs supported on acid supports. In this article we detailed our studies on the stabilization of small (<10 nm) Au NPs on multifunctional nanomaterials comprised of magnetite NPs coated by silica and its use to catalyze the selective oxidation of multifunctional alcohols to unsaturated aldehydes or ketones. The Au NPs could only be stabilized and firmly attached to support surfaces that were previously modified with amino groups. The metal-support interactions before and after the Au NPs formation were observed by X-ray absorption fine structure spectroscopy (XAFS).

Results and Discussion

Impregnation of gold(III) ions on the catalyst support: The multifunctional magnetic nanomaterial used as catalyst support in this study was synthesized following the procedure described by Jacinto and co-workers,^[34] and consists of superparamagnetic magnetite NPs spherically coated with silica by a microemulsion technique. In the impregnation step, the magnetic solid was added to an aqueous solution of gold(III) chloride at pH ≈ 6 for spontaneous attachment of gold(III) ions on its surface; however, the loading of the anionic gold species $[\text{Au}(\text{OH})_x\text{Cl}_{4-x}]^-$ on the surface of silica was very low. This was expected because the negatively charged silica surface (zero potential charge (ZPC) ≈ 2), and is in agreement with previously reported results.^[47,48] The catalyst support, named $\text{Fe}_3\text{O}_4@\text{SiO}_2$, was further modified by 3-(aminopropyl)triethoxysilane (APTES) to prepare $\text{Fe}_3\text{O}_4@\text{SiO}_2\text{-NH}_2$. This amino-modified solid, when treated with an aqueous solution of gold(III) chloride at pH ≈ 6, was readily loaded with 0.72 wt % of gold, as determined by inductively coupled plasma optical emission spectrometry (ICP OES). The nonfunctionalized $\text{Fe}_3\text{O}_4@\text{SiO}_2$, on the other hand, could only be loaded with gold(III) ions by wet impregnation, which means that a nominal 0.72 wt % gold loading was obtained by adding a small volume of an aqueous solution of gold(III) chloride at pH ≈ 6 to the nonfunctionalized solid followed by evaporation of the solvent.

This first set of experiments confirmed the very low affinity of the silica surfaces for gold(III) ions and that the impregnation process on the amino-functionalized solid is most probably favored by the coordination of the gold ions to the amino groups rather than to adsorption to the support surfaces.

X-ray absorption fine structure (XAFS) spectroscopy of gold on silica: To better distinguish the coordination of gold ions to the amino groups or their adsorption onto the support surface, the electronic properties of the gold species were investigated by X-ray absorption near edge structure (XANES) analysis. The XANES spectra can be used to evaluate the average oxidation state of the absorbing atom in the sample. Complementary data was obtained by the

analysis of the extended X-ray absorption fine structure (EXAFS). These studies were performed by using model systems composed of silica spheres synthesized by a sol-gel method,^[49] instead of silica-coated magnetic NPs. The silica nanospheres were treated with APTES to prepare the catalyst support, named $\text{SiO}_2\text{-NH}_2$, or were used as-prepared, named SiO_2 . Both samples were treated with gold(III) chloride aqueous solution at pH ≈ 6, as previously described for the magnetic support. Figure 1 shows the XANES spectra of

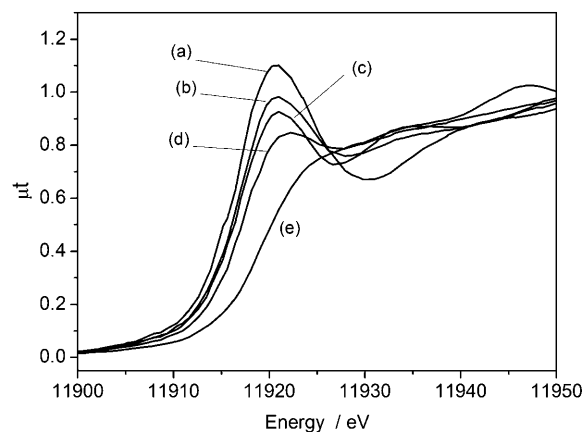


Figure 1. XANES spectra at the Au L_3 -edge: a) $\text{Au}(\text{CH}_3\text{COO})_3$, b) $\text{SiO}_2\text{-Au}^{3+}$, c) HAuCl_4 , d) $\text{SiO}_2\text{-NH}_2\text{-Au}^{\sigma+}$ and e) Au foil.

the samples ($\text{SiO}_2\text{-Au}$ and $\text{SiO}_2\text{-NH}_2\text{-Au}$) and the standards (Au foil, HAuCl_4 , and $\text{Au}(\text{CH}_3\text{COO})_3$). The intense white line at 11920 eV is characteristic of Au^{3+} and the difference of intensity in the case of $\text{Au}(\text{CH}_3\text{COO})_3$ (Figure 1a) and HAuCl_4 (Figure 1c) can be related to the coordination of gold to different groups. The XANES spectrum of gold loaded on the nonfunctionalized silica (Figure 1b) exhibits an intermediate white line intensity, which suggests the interaction of the Au^{3+} species with the oxygenate species on the silica surface. More interesting, the white line intensity of gold loaded on the amino-functionalized silica (Figure 1d) decreased relative to HAuCl_4 , indicating a partial reduction of Au^{3+} to $\text{Au}^{\sigma+}$ species, most probably Au^{1+} .^[50] Figure 2 shows the Fourier transform of the EXAFS oscillations with the best fit for the first coordination shell. The results are presented in Table 1. The only variables in the fit

Table 1. EXAFS results.

Sample	Shell	N	r [Å]	σ^2 [Å ²]	ΔE°
Au-foil	Au-Au	12	2.88 (1)	0.008 (0)	7.7 (4)
HAuCl_4	Au-Cl	4	2.27 (1)	0.002 (1)	7 (1)
$\text{Au}(\text{CH}_3\text{COO})_3$	Au-O	3.7 (5) ^[a]	1.97 (1)	0.002 (2)	8 (2)
$\text{SiO}_2\text{-NH}_2\text{-Au}^{\sigma+}$	Au-Cl	1.3 (5)	2.27 ^[b]	0.002 ^[b]	7 ^[b]
	Au-O/N	1.6 (5)	1.97 ^[b]	0.002 ^[b]	8 ^[b]
$\text{SiO}_2\text{-Au}^{3+}$	Au-Cl	2.0 (5)	2.27 ^[b]	0.002 ^[b]	7 ^[b]
	Au-O	1.7 (5)	1.97 ^[b]	0.002 ^[b]	8 ^[b]

[a] For octahedral coordination, $N_{\text{Au-O}}=6$. The presented value was found experimentally to our standard. [b] The experimental values found for the standards were kept fixed for the samples.

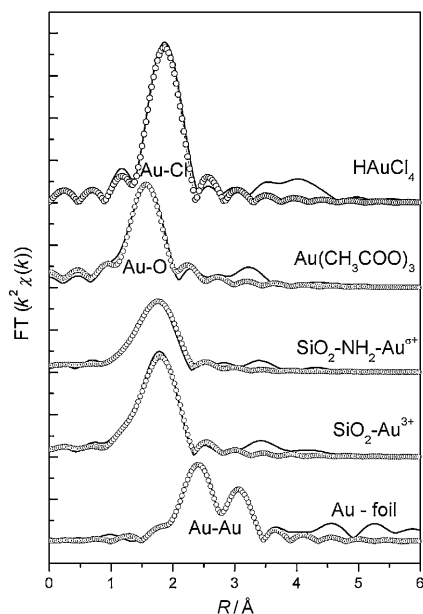


Figure 2. Fourier transform of the EXAFS oscillations for the $\text{SiO}_2\text{-Au}^{3+}$ and $\text{SiO}_2\text{-NH}_2\text{-Au}^{\sigma+}$ solids and standards ($\text{Au}(\text{CH}_3\text{COO})_3$, HAuCl_4 and Au foil).

of the $\text{SiO}_2\text{-NH}_2\text{-Au}^{\sigma+}$ and $\text{SiO}_2\text{-Au}^{3+}$ solids were the Au-Cl and Au-O/N coordination numbers ($N_{\text{Au-Cl}}$ and $N_{\text{Au-O/N}}$), interatomic distances ($r_{\text{Au-Cl}}$ and $r_{\text{Au-O/N}}$), Debye–Waller factors ($\sigma_{\text{Au-Cl}}^2$ and $\sigma_{\text{Au-O/N}}^2$), energy shifts ($\Delta E_{\text{Au-Cl}}^0$ and $\Delta E_{\text{Au-O/N}}^0$), and inelastic loss amplitude correction (S_0^2) were found for the standards and kept fixed to decrease the number of parameters to fit. It is important to point out that it is not possible to distinguish between N and O from EXAFS, since they have similar phase shifts and scattering amplitudes.^[51] EXAFS analyses show a decrease in the Au-Cl coordination in both samples. This is slightly more accentuated for the $\text{SiO}_2\text{-NH}_2\text{-Au}^{\sigma+}$ sample, which is in agreement with the more significant change in the XANES spectrum. The $N_{\text{Au-O/N}}$ average value is similar in both samples, which reinforces that the differences found in XANES spectra are related to a specific interaction with the amino groups that takes place in the $\text{SiO}_2\text{-NH}_2\text{-Au}^{\sigma+}$ sample. As pointed out before, the XANES spectrum of $\text{SiO}_2\text{-Au}^{3+}$ exhibits an intermediate white line intensity (more intense than HAuCl_4), which suggests the interaction of the Au^{3+} species with the oxygenate species on the silica surface. On the other hand, the white line intensity of $\text{SiO}_2\text{-NH}_2\text{-Au}^{\sigma+}$ decreased relative to HAuCl_4 , indicating a partial reduction of Au^{3+} to $\text{Au}^{\sigma+}$ species, most probably Au^{1+} . The plausible reason for this, since we have used exactly the same silica (with and without functionalization with amino groups), should be the presence of the amino groups. Transmission electron microscopy (TEM) analysis (see below) confirmed that the Au NPs formed after reduction are more firmly attached to the amino-functionalized solid, which support the XAFS evidences that the NH_2 functional groups grafted on the support surface interact more strongly with the metal ions than the

silanol groups present on the surfaces of the nonfunctionalized support.

Synthesis and characterization of supported Au NPs: The supported Au NPs were prepared by reduction of the gold species loaded on the support. As discussed in our previous paper,^[52] the gold precursor can be reduced either by thermal treatment or by molecular hydrogen gas. Reduction with H_2 gives a narrower particle size distribution. Therefore, the solids, $\text{Fe}_3\text{O}_4\text{@SiO}_2\text{-NH}_2\text{-Au}^{\sigma+}$ and $\text{Fe}_3\text{O}_4\text{@SiO}_2\text{-Au}^{3+}$, were both dispersed in cyclohexane and submitted to H_2 gas under controlled mild conditions to give supported Au NPs. The morphology of the solids was examined by TEM and the images are shown in Figure 3. The Au NPs

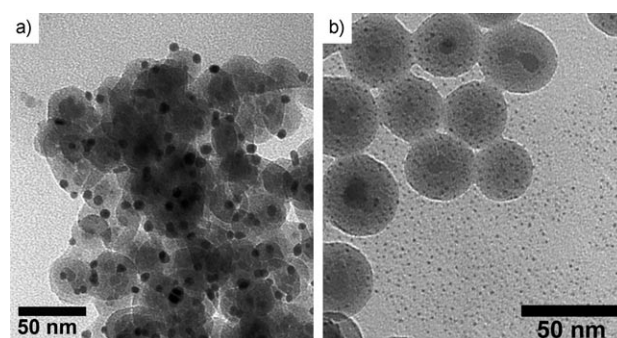


Figure 3. TEM images of a) $\text{Fe}_3\text{O}_4\text{@SiO}_2\text{-NH}_2\text{-Au}^0$ and b) $\text{Fe}_3\text{O}_4\text{@SiO}_2\text{-Au}^0$.

supported on the amino-functionalized solid $\text{Fe}_3\text{O}_4\text{@SiO}_2\text{-NH}_2\text{-Au}^0$ (Figure 3 a) were well-dispersed and exclusively attached to the silica layer. The histogram of Au NPs size distribution was fitted to a LogNormal function with mean diameter of 5.9 nm ($\sigma=0.18$).^[52] When an aqueous suspension of the $\text{Fe}_3\text{O}_4\text{@SiO}_2\text{-NH}_2\text{-Au}^0$ solid is submitted to magnetic separation, a supernatant solution completely free of gold is recovered. On the other hand, the Au NPs reduced on the nonfunctionalized solid were not firmly attached to the silica layer and could be seen in different regions of the TEM grid (Figure 3 b). Moreover, during the washing procedure and sample preparation, the supernatant aqueous solution was colored by Au NPs transferred from the surface of the magnetic solid to the liquid phase because of the weak interaction between the support and the NPs.

The samples of silica prepared for the XAFS analysis were also reduced by hydrogen gas. The XANES spectra of the reduced samples (see Figure S1, Supporting Information) are similar to the Au foil standard. The EXAFS analysis (see Figure S2 and Table S1, Supporting Information) gives coordination numbers close to Au bulk in agreement with TEM images that shows the formation of Au NPs with average size > 5 nm.

Oxidation of multifunctional alcohols to aldehydes and ketones: The catalytic properties of the magnetically recoverable $\text{Fe}_3\text{O}_4\text{@SiO}_2\text{-NH}_2\text{-Au}^0$ catalyst were first demonstrated

by using benzyl alcohol as a model substrate.^[52] The catalyst was highly active, selective to the aldehyde product, and very efficiently recovered by magnetic separation with negligible Au leaching to the solution. In the present study, the oxidation of multifunctional alcohols was initially tested for the aerobic oxidation of cinnamyl alcohol and then expanded to other substrates. As for benzyl alcohol oxidation, the catalytic reaction did not proceed without base (Figure 4). This is in agreement with the proposed oxidation

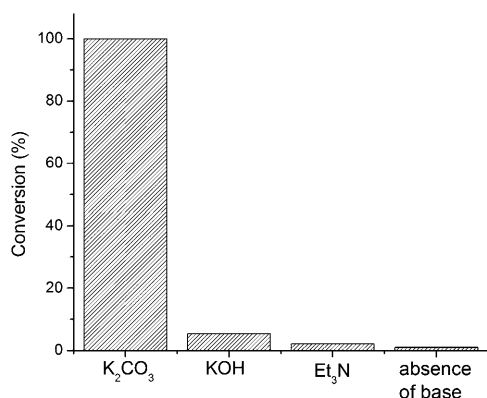


Figure 4. Oxidation of cinnamyl alcohol by the magnetically recoverable Fe₃O₄@SiO₂-NH₂-Au⁰ catalyst in the absence and in the presence of different bases. Conditions: substrate (2 mmol), supported catalyst (50 mg, 2.54 μmol Au), base, toluene (2 mL), 110 °C, O₂ at 3 atm, 6 h.

mechanism through an initial hydrogen-abstraction pathway.^[29] Different bases were tested and potassium carbonate has shown the best conversion of cinnamyl alcohol to cinnamyl aldehyde (Figure 4). Potassium hydroxide caused corrosion of the silica layer (see Figure S3, Supporting Information) and very low conversion of the substrate, and triethylamine (Et₃N) caused metal leaching and catalyst deactivation. ICP-OES analysis of the products isolated by magnetic separation showed negligible amounts of gold for the reaction without base, with potassium hydroxide and with potassium carbonate; however, a large amount of gold was transferred to the liquid phase for the reaction with Et₃N. The concentration of gold in the liquid phase after reaction was 0.175 mg ml⁻¹, which corresponds to 97% of the gold added to the reaction medium.

The control experiment in the absence of metal (only with the Fe₃O₄@SiO₂-NH₂) under the same reaction conditions given in Figure 4 showed no conversion of benzyl alco-

hol, even in the presence of K₂CO₃, so the support alone has no effect on the oxidation reaction.

A variety of multifunctional alcohols were converted to the corresponding aldehydes and ketones with good yield and selectivity as summarized in Table 2. The catalyst was highly selective for the oxidation of alcohols containing C=C double bonds. As can be observed in Table 2 (entry 6–8), primary and secondary α,β-unsaturated alcohols were selectively oxidized to the corresponding unsaturated aldehydes or ketones without the occurrence of unexpected side reactions, such as intramolecular hydrogen transfer, *cis,trans*-isomerization, epoxidation, or polymerization of the C=C bond.

It is important, when working with heterogeneous systems, to determine whether or not leaching of gold occurs. To address this point the isolated solution containing the products, obtained after magnetic separation of the solid catalyst, was analyzed by atomic absorption spectroscopy, whereby the presence of gold could not be detected (less than 2.5 ppb of Au, limit of quantitation by ICP OES).

The catalytic activity of the catalyst precursor containing Au^{σ+} species on the surface of the support (not reduced by H₂) was tested and gives good conversion of benzyl as well as cinnamyl alcohol. The oxidation reaction was accompanied by changes in the color of the catalyst that suggest in situ reduction of the Au^{σ+} species to Au⁰ NPs. TEM analysis of the material isolated after the catalytic reaction showed

Table 2. Oxidation of alcohols by the magnetically recoverable, Au NP catalyst.

Entry ^[a]	Substrate	Product	<i>p</i> O ₂ [atm]	Conversion ^[b]	Selectivity ^[b]
1			5	95.7	100
2			5	78.2	99.5
3			5	73.4	97
4			6	4.3	100
5			4	99.8	100
6			4	99.0	99.0
7			6	64.1	99.0
8			4	99.0	99.0

[a] Reaction condition: substrate (2 mmol), supported catalyst (50 mg, 2.54 μmol Au), K₂CO₃ (50 mg), toluene (2 mL), 110 °C, 6 h. [b] Determined by GC.

that Au NPs were formed; however, the particles have a broad particle size distribution in the range of 2.1 to 31 nm (see Figure S4, Supporting Information). Therefore, the reduction step with hydrogen is important to control the particles size of the Au NPs and should not be eliminated in the preparation of this catalyst.

Conclusion

The preparation of Au NPs supported on silica is not straightforward. The impregnation process is very limited in neutral pH, but could be improved by the functionalization of the silica surfaces. Amino-functionalized silica surfaces allowed the stabilization of ≈ 6 nm Au NPs on the surface of a multifunctional, silica-based, magnetic support that presented catalytic activity and selectivity for the oxidation of multifunctional alcohols, while it rendered isolation of the spent catalyst by magnetic separation. XANES analysis characterized the catalyst precursor Au^{III} species and the supported Au^0 NPs, giving evidence that the NH_2 functional groups grafted on the support surface interact more strongly to the metal ions than simple metal adsorption on the surfaces of nonfunctionalized support.

Experimental Section

Synthesis of silica-coated magnetite nanoparticles: The core-shell $\text{Fe}_3\text{O}_4/\text{SiO}_2$ composite was prepared by means of a microemulsion formulation reported elsewhere.^[34] The solid was used as-prepared or modified with amino groups by reaction with 3-aminopropyltriethoxysilane (APTES) in dry toluene under N_2 , to give the amino-functionalized solid support ($\text{Fe}_3\text{O}_4/\text{SiO}_2\text{-NH}_2$).

Synthesis of supported Au^0 NPs: $\text{Fe}_3\text{O}_4/\text{SiO}_2\text{-NH}_2$ (500 mg) was added to an aqueous solution of HAuCl_4 (100 mL, 1 g L^{-1}) with pH 6. The mixture was kept under stirring at 25°C for two hours. The solid was then magnetically collected from the solution and washed twice with hot distilled water. The reduction step was performed in a Fischer–Porter glass reactor pressurized with hydrogen gas. The gold precursor was dispersed in cyclohexane and heated to 80°C under H_2 at 4 atm. The mixture was stirred for 3 h and the color of the solid changed from brown to dark purple.

Catalytic experiments: In a typical experiment, $\text{Fe}_3\text{O}_4/\text{SiO}_2\text{-NH}_2\text{-Au}^0$ (50 mg of solid, $2.54 \mu\text{mol Au}$), K_2CO_3 (50 mg, 0.5 mmol), and toluene (2 mL) containing the desired quantity of substrate (2.0 mmol) were added to a Fischer–Porter glass reactor. The reactor was evacuated and loaded with O_2 to the desired pressure. The reaction was conducted under magnetic stirring (700 rpm) and the temperature was maintained by an oil bath on a hot-stirring plate connected to a digital controller (ETS-D4 IKA). After the desired time, the catalyst was recovered magnetically and the liquid phase was collected and analyzed by gas chromatography (GC) and GC-MS.

Materials and methods

XAFS analysis: X-ray absorption fine structure spectroscopy (XAFS) was performed at the XAFS1 beamline of the LNLS (Campinas, Brazil). The measurements were performed in transmission mode at the Au L_3 -edge (11920 eV) and the samples were prepared as pellets. The EXAFS data were analysed using Athena/Artemis software packages and standard procedures ($k_{\text{max}} = 10 \text{ \AA}^{-1}$).^[53]

TEM analysis: The morphology of the Au NPs was obtained on a Philips CM 200 microscope operating at an accelerating voltage of 200 kV. The samples for TEM were prepared by collecting a small portion of nanoparticles dispersed in an aqueous solution on a carbon-coated copper grid. The histogram of nanoparticles size distribution was obtained from the measurement of about 450 particles found in an arbitrarily chosen area of enlarged micrographs.

GC-MS analysis: Gas chromatography analyses were performed on a Shimadzu GCMS-QP5050 A, equipped with a 30 m capillary column with 5% phenyl-95% dimethylpolysiloxane stationary phases (AT5), using the following parameters: initial temperature: 40°C , temperature ramp:

5°C min^{-1} (from 40 to 150°C), and $40^\circ\text{C min}^{-1}$ (from 150 to 250°C), final temperature: 250°C , injection volume: $1 \mu\text{L}$. The products were quantified using internal calibration (undecane).

ICP-OES analysis: The gold content in the solid catalyst and in the oxidation products was measured using an inductively coupled plasma optical emission spectrometer Genesis SOP (Spectro). Reference solutions of Au (1000 mg L^{-1}) with a high degree of analytical purity (ICP Standard, SpecSol) were used to obtain the calibration curves. Deionized water (MILLI-Q) was used to prepare all solutions. The sample digestion was carried out at 100°C for 3 h with aqua regia (5 mL). For liquid samples, the organic phase was previously evaporated. The volume of the samples was then adjusted to 25 mL using DI water. The gold content was quantified in duplicate for each sample.

Acknowledgements

The authors are grateful to the Brazilian agencies FAPESP and CNPq for financial support and indebted to the Laboratório Nacional de Luz Síncrotron (LNLS) (Campinas, Brazil) for use of XAFS1 beamline. The authors also acknowledge the Instituto Nacional de Ciência e Tecnologia de Catalise em Sistemas Moleculares e Nanoestruturados (INCT-Catalise).

- [1] M. Hudlicky, *Oxidations in Organic Chemistry*, American Chemical Society, Washington, DC, **1990**.
- [2] R. A. Sheldon, *Green Chem.* **2007**, *9*, 1273–1283.
- [3] K. Kaneda, M. Fujii, K. Morioka, *J. Org. Chem.* **1996**, *61*, 4502–4503.
- [4] P. Nagaraju, M. Balaraju, K. M. Reddy, P. S. S. Prasad, N. Lingaiah, *Catal. Commun.* **2008**, *9*, 1389–1393.
- [5] S. H. Liu, G. K. Chuah, S. Jaenicke, *J. Mol. Catal. A* **2004**, *220*, 267–274.
- [6] T. Nakano, Y. Ishii, M. Ogawa, *J. Org. Chem.* **1987**, *52*, 4855–4859.
- [7] L. Tonucci, M. Nicastro, N. d'Alessandro, M. Bressan, P. D'Ambrósio, A. Morvillo, *Green Chem.* **2009**, *11*, 816–820.
- [8] S. Yamazaki, Y. Yamazaki, *Chem. Lett.* **1989**, *18*, 1361–1364.
- [9] J. Liu, F. Wang, R. Dewil, *Catal. Lett.* **2009**, *130*, 448–454.
- [10] K. Ebitani, H.-B. Ji, T. Mizugaki, K. Kaneda, *J. Mol. Catal. A* **2004**, *212*, 161–170.
- [11] M. Besson, P. Gallezot, *Catal. Today* **2000**, *57*, 127–141.
- [12] Y. Kon, Y. Usui, K. Sato, *Chem. Commun.* **2007**, 4399–4400.
- [13] A. F. Lee, J. J. Gee, H. J. Theyers, *Green Chem.* **2000**, *2*, 279–282.
- [14] A. Corma, H. Garcia, *Chem. Soc. Rev.* **2008**, *37*, 2096–2126.
- [15] A. Abad, ; A. Corma, ; H. García, *Chem. Eur. J.* **2008**, *14*, 212–222
C. Almela, A. Corma, H. Garcia, *Chem. Commun.* **2006**, 3178–3180.
- [16] C. Della Pina, E. Falleta, L. Patri, M. Rossi, *Chem. Soc. Rev.* **2008**, *37*, 2077–2095.
- [17] A. Abad, ; A. Corma, ; H. García, *Chem. Eur. J.* **2008**, *14*, 212–222.
- [18] A. S. K. Hashmi, G. J. Hutchings, *Angew. Chem.* **2006**, *118*, 8064–8105; *Angew. Chem. Int. Ed.* **2006**, *45*, 7896–7936.
- [19] F. Porta, L. Prati, *J. Catal.* **2004**, *224*, 397–403.
- [20] D. Abad, P. Conception, A. Corma, H. Garcia, *Angew. Chem.* **2005**, *117*, 4134–4137; *Angew. Chem. Int. Ed.* **2005**, *44*, 4066–4069.
- [21] A. Abad, C. Almela, A. Corma, H. Garcia, *Tetrahedron* **2006**, *62*, 6666–6672.
- [22] D. Enache, D. W. Knight, G. J. Hutchings, *Catal. Lett.* **2005**, *103*, 43–52.
- [23] D. Enache, J. K. Edwards, P. Landon, B. Solsona-Espriu, A. F. Carley, A. A. Herzing, M. Watanabe, C. J. Kiely, D. W. Knight, G. J. Hutchings, *Science* **2006**, *311*, 362–365.
- [24] V. R. Choudhary, A. Dhar, P. Jana, R. Jha, B. S. Uphade, *Green Chem.* **2005**, *7*, 768–770.
- [25] P. Haider, A. Baiker, *J. Catal.* **2007**, *248*, 175–187.
- [26] C. Milone, R. Ingoglia, G. Neri, A. Pistone, S. Galvagno, *Appl. Catal. A* **2001**, *211*, 251–257.

- [27] A. N. Pestryakov, V. V. Lunin, *J. Mol. Catal. A* **2000**, *158*, 325–329.
- [28] J. Hu, L. Chen, K. Zhu, A. Suchopar, R. Richards, *Catal. Today* **2007**, *122*, 277–283.
- [29] S. Carrettin, P. McMorn, P. Johnston, K. Griffin, G. J. Hutchings, *Chem. Commun.* **2002**, 696–697.
- [30] G. J. Hutchings, S. Carrettin, P. Landon, J. K. Edwards, D. Enache, D. W. Knight, Y.-J. Xu, A. F. Carley, *Top. Catal.* **2006**, *38*, 223–230.
- [31] S. Biella, G. L. Castiglioni, C. Fumagalli, L. Prati, M. Rossi, *Catal. Today* **2002**, *72*, 43–49.
- [32] L. M. Rossi, F. P. Silva, L. L. R. Vono, P. K. Kiyohara, E. L. Duarte, R. Itri, R. Landers, G. Machado, *Green Chem.* **2007**, *9*, 379–385.
- [33] L. M. Rossi, I. M. Nangoi, N. J. S. Costa, *Inorg. Chem.* **2009**, *48*, 4640–4642.
- [34] M. J. Jacinto, P. K. Kiyohara, S. H. Masunaga, R. F. Jardim, L. M. Rossi, *Appl. Catal. A* **2008**, *338*, 52–57.
- [35] M. J. Jacinto, O. H. C. F. Santos, R. F. Jardim, R. Landers, L. M. Rossi, *Appl. Catal. A* **2009**, *360*, 177–182.
- [36] M. J. Jacinto, R. Landers, L. M. Rossi, *Catal. Commun.* **2009**, *10*, 1971–1974.
- [37] P. D. Stevens, G. Li, J. Fan, M. Yen, Y. Gao, *Chem. Commun.* **2005**, 4435–4437.
- [38] M. Kotani, T. Koibe, K. Yamaguchi, N. Mizuno, *Green Chem.* **2006**, *8*, 735–741.
- [39] A. Hu, G. T. Yee, W. Lin, *J. Am. Chem. Soc.* **2005**, *127*, 12486–12487.
- [40] N. Zheng, G. D. Stucky, *J. Am. Chem. Soc.* **2006**, *128*, 14278–14280.
- [41] F. Porta, L. Prati, M. Rossi, S. Coluccia, G. Martra, *Catal. Today* **2000**, *61*, 165–172.
- [42] G.-H. Wang, W.-C. Li, K.-M. Jia, B. Spliethoff, F. Schüth, A.-H. Lu, *Appl. Catal. A* **2009**, *364*, 42–47.
- [43] R. L. Oliveira, P. K. Kiyohara, L. M. Rossi, *Green Chem.* **2009**, *11*, 1366–1370.
- [44] G. Martra, L. Prati, C. Manfredotti, S. Biella, M. Rossi, S. Coluccia, *J. Phys. Chem. B* **2003**, *107*, 5453–5459.
- [45] M. Okumura, S. Tsubota, M. Haruta, *J. Mol. Catal. A* **2003**, *199*, 73–84.
- [46] S. Arrii, F. Morfin, A. J. Renouprez, J. L. Rousset, *J. Am. Chem. Soc.* **2004**, *126*, 1199–1205.
- [47] R. Zanella, A. Sandoval, P. Santiago, V. A. Basiuk, J. M. Saniger, *J. Phys. Chem. B* **2006**, *110*, 8559–8565.
- [48] N. Phonthammachai, T. J. White, *Langmuir* **2007**, *23*, 11421–11424.
- [49] L. M. Rossi, L. Shi, F. H. Quina, Z. Rosenzweig, *Langmuir* **2005**, *21*, 4277–4280.
- [50] C. K. Costello, J. Guzman, J. H. Yang, Y. M. Wang, M. C. Kung, B. C. Gates, H. H. Kung, *J. Phys. Chem. B* **2004**, *108*, 12529–12536.
- [51] J. E. Penner-Hahn, *Coord. Chem. Rev.* **1999**, *190–192*, 1101–1123.
- [52] R. L. Oliveira, P. K. Kiyohara, L. M. Rossi, *Green Chem.* **2010**, *12*, 144–149.
- [53] B. Ravel, M. Newville, *J. Synchrotron Radiat.* **2005**, *12*, 537–541.

Received: August 5, 2010

Revised: October 27, 2010

Published online: February 24, 2011